Colloid Polym Sci (2008) 286:267–274
DOI 10.1007/s00396-007-1765-y

ORIGINAL CONTRIBUTION

Preparation and characterization of side-chain liquid crystalline polymers containing chenodeoxycholic acid residue

Wenqiang Xiao · Baoyan Zhang · Yuehua Cong

Received: 8 June 2007 / Revised: 29 July 2007 / Accepted: 15 August 2007 / Published online: 28 September 2007

Abstract A series of new side-chain liquid crystalline polymers containing chenodiol residue derived from 24-[4′-hydroxybiphenyl-4-yl-4-(allyloxy)benzoyloxy]-3α, 7α-di{*n*-[4′-(4-ethoxybenzoyloxy)biphenyl-4-yloxy]-*n*-oxoalkanoyloxy}-5β-cholane was designed and prepared. The chemical structures of the monomer and polymer were confirmed by Fourier transform infrared and ^{1}H NMR spectra. The mesomorphic properties of monomer and polymer were investigated by differential scanning calorimetry, thermogravimetric analysis, polarizing optical microscopy, and X-ray diffraction. The side-chain liquid crystalline polymers revealed wide mesophase temperature range and high thermal stability, and they showed nematic liquid crystalline phase. The influence of flexible space group length on thermal properties and specific rotation was examined.

Keywords Preparation · Liquid crystalline polymers · Nematic phase · Chenodeoxycholic acid · Threadlike texture

Introduction

Side-chain liquid crystalline polymers (LCPs) are an attractive class of compounds combining liquid crystalline properties with polymer properties such as thermal stability and processability [1–10]. These properties make side-chain LCPs potential candidates for technological applications, such as in the fields of optical storage [11], dynamic holography [12], liquid-crystal command surfaces [13], nonlinear optical devices [14], light-emitting diodes [15], and molecular switches [16].

The side-chain LCPs containing cholesteryl mesomorphic group can form wonderful cholesteric liquid crystalline phase [17–22]. The chenodeoxycholic acid and cholesterol belong to sterol compound, and they have similar molecular structure. In previous studies, the chenodeoxycholic acid was mainly used to synthesize a series of compounds, which were applied for biology [23, 24]. However, in marked contrast to the extensive studies of side-chain liquid crystalline polymers containing cholesteryl, very few cases of side-chain liquid crystalline polymers containing chenodiol have been reported. Therefore, it is of application and theoretical interest to design and synthesize a series of liquid crystalline monomers containing chenodeoxycholic acid group, and then liquid crystalline polymers are prepared by radical polymerization. The chemical structures and mesomorphic properties of the monomer and polymer were characterized with Fourier transform infrared (FIR), proton nuclear magnetic resonance (^{1}H NKr), differential scanning calorimetry (DSC), thermogravimetric analysis (TGA), polarizing optical microscopy (POM), specific rotation (SROT), and X-ray diffraction (XRD).

Experimental

Materials

Chenodeoxycholic acid was purchased from Huainan Biochemistry Industry Limited Company (China).

W. Xiao · B. Zhang (✉)
The Research Centre for Molecular Science and Engineering,
Northeastern University,
Shenyang 110004, People's Republic of China
e-mail: baoyanzhang@hotmail.com

Y. Cong
School of Chemistry, Cardiff University,
Cardiff, UK

1-Bromopropene, Diacid, and AIBN (azo-bis-isobutyronitrile) were purchased from Beijing Jinlong Chemical Reagent (China). 4-Hydroxybenzoic acid, 4,4′-dihydroxydiphenyl, and 4-ethoxybenzoic acid were purchased from Beijing Fuxing Chemical Industry (China). Toluene was first refluxed over sodium and then distilled. All other solvents and reagents were purified by standard methods.

Characterization

Fourier transform infrared (FTIR) spectra were measured on a spectrum one (B) spectrometer (PerkinElmer, Foster City, CA, USA). ^{1}H NMR spectra (300 MHz) were obtained using a Gemini 300 spectrometer (Varian Associates, Palo Alto, CA, USA). Specific rotations were measured on a PerkinElmer 341 polarimeter. Phase transition temperatures and thermodynamic parameters were determined using a DSC 204 (Netzsch, Hanau, Germany) equipped with a liquid nitrogen cooling system. The heating and cooling rates were 10 °C/min. A DMRX POM instrument (Leica, Germany) equipped with a THMSE-600 hot stage (Linkam, England) was used to observe phase-transition temperatures and analyze liquid crystalline properties through the observation of optical texture. XRD measurements were performed using nickel-filtered Cu-K_α (λ=1.542 Å) radiation with a DMAX-3A powder diffractometer (Rigaku, Tokyo, Japan). Dilute solution viscosity measurements were carried out in pyridine solution at 30±0.2 °C, using an Ubbelohde capillary viscometer. The flow times were kept sufficiently long (>100 s), so that kinetic energy corrections could be neglected.

Synthesis of the monomers

The synthetic route of monomers is shown in Scheme 1. Due to the similarity of synthesis, the method to synthesize monomer 24-[4′-hydroxybiphen-yl-4-yl-4(allyloxy) benzoyloxy]-3α,7α-di{6-[4′-(4ethoxybenzoyloxy)biphenyl-

Scheme 1 Synthetic route of the monomers

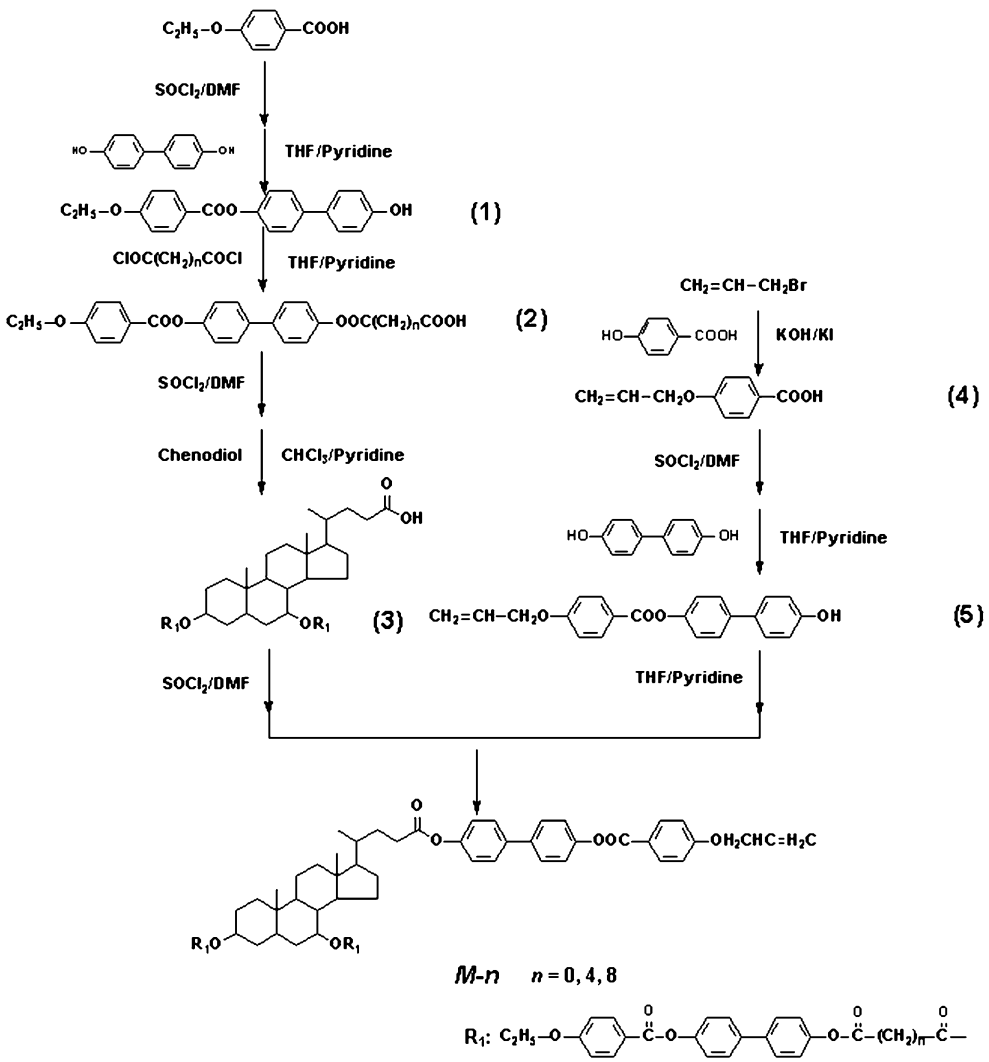

4-yloxy]-6-oxohexanoyloxy}-5β-cholane (*M-n*, n = 4) is reported here as general procedure.

4′ − hydroxybiphenyl − 4 − yl − ethoxybenzoate (1)

4-Ethoxybenzoic acid (8.3 g, 0.05 mol) reacted at 60 °C with thionyl chloride (25 ml) containing a few drops of *N*, *N*-dimethylformamide (DMF) for 6 h. The excess thionyl chloride was removed under reduced pressure to give the corresponding acid chloride. The acid chloride was dissolved in tetrahydrofuran (THF) (10 ml) and dropped into THF (200 ml) solution of 4,4′-dihydroxybiphenyl (55.8 g, 0.3 mol) under quick stirring; the dry pyridine (20 ml) as a catalyst was added. The reaction mixture was refluxed for 15 h. After removal of the excess solvent, the residue was poured into water and neutralized with dilute hydrochloric acid. The crude product was obtained by filtration and washed with dilute sodium hydroxide solution, dilute hydrochloric acid, and cold ethanol successively. The white solid 1 was obtained by recrystallization with acetone (mp: 220 °C, yield: 62%). IR (KBr, cm^{-1}): 3,443 (–OH); 2,983; 2,850 (–CH_2–); 1701 (C=O); 1,609; 1497 (–Ar); 1,264 (C–O–C). ^{1}H NMR ($CDCl_3$): 1.30 (m, 3H, –CH_3), 3.98 (m, 2H, –OCH_2–), 6.79–8.03 (m, 12H, Ar*H*), 9.33 (s, 1H, –O*H*).

6 − [4′ − (4 − ethoxybenzoyloxy)biphenyl − 4 − yloxy] − 6 − oxohexanoicacid (2)

Compound 4′-hydroxybiphenyl-4-yl-4-ethoxybenzoate (3.34 g, 0.01 mol) was dissolved in THF (100 ml), and then added into a solution containing adipic chloride (8.76 g, 0.06 mol), THF (80 ml), and dry pyridine (12 ml). The reaction mixture was refluxed for 16 h. After cooling back to room temperature, the mixture was poured into cold water and acidified with hydrochloric acid. The precipitate was recrystallized from ethanol, and then product was dried in a vacuum oven to achieve a white solid 2 (mp: 178 °C, yield: 68%). IR (KBr, cm^{-1}): 3,075 (–OH); 2,977; 2,852 (–CH_2–); 1,751; 1,731 (C=O); 1604; 1492 (–Ar); 1261 (C–O–C). ^{1}H NMR ($CDCl_3$): 1.33 (m, 3H, –CH_3), 3.99 (m, 2H, –OCH_2–), 7.07–8.01 (m, 12H, Ar*H*), 1.46–2.24 (m, 8H, *H*–Adipoyl), 12.11 (s, 1H, –O*H*).

3α, 7α − di{6−[4′−(4 − ethoxybenzoyloxy)biphenyl − 4 − yloxy] − 6 − oxohexanoyloxy} − 5β − cholan − 24 − oic acid (3)

Compound 2 (2.0 g, 4.3 mmol) was stirred in thionyl chloride (30 ml) and DMF (0.1 ml) as a catalyst was added. The solution was refluxed for 5 h whereby a clear solution was obtained. The excess of thionyl chloride was removed in vacuum for 4 h. The obtained acid chloride was dissolved in dry chloroform (30 ml), then dry pyridine (0.1 ml) and anhydrous chenodeoxycholic acid (0.84 g, 2.13 mmol) was added. The reaction mixture was refluxed for 16 h under a nitrogen atmosphere. After cooling back to room temperature, the mixture was poured into cold water (100 ml) and acidified with hydrochloric acid. The precipitate was collected by filtration and washed with distilled water. The pure compound 3α,7α-di{6-[4′-(4-ethoxybenzoyloxy)biphenyl-4-yloxy]-6-oxohexanoyloxy}-5β-cholan-24-oic acid 3 was obtained while hot to filter in acetone (mp: 205 °C, yield: 70%). IR (KBr, cm^{-1}): 2,936; 2,849 (–CH_2–); 2,815 (–COOH); 1,748 (–RCOOAr–); 1,729 (–ArCOOAr–); 1,605 (–Ar); 1254 (C–O–C). ^{1}H NMR ($CDCl_3$): 1.37 (m, 6H, –CH_3), 4.04 (m, 4H, –OCH_2–), 7.11 (d, 4H, J = 5.3Hz, –O–Ar*H*–COO–), 8.17 (d, 4H, J = 1.3Hz, –O–Ar*H*–COO–), 7.14–7.61 (m,

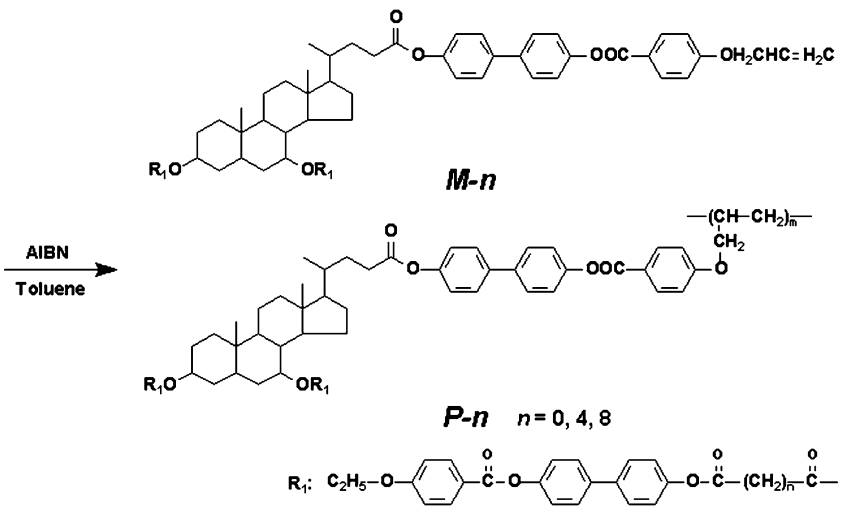

Scheme 2 Synthetic route of the polymers

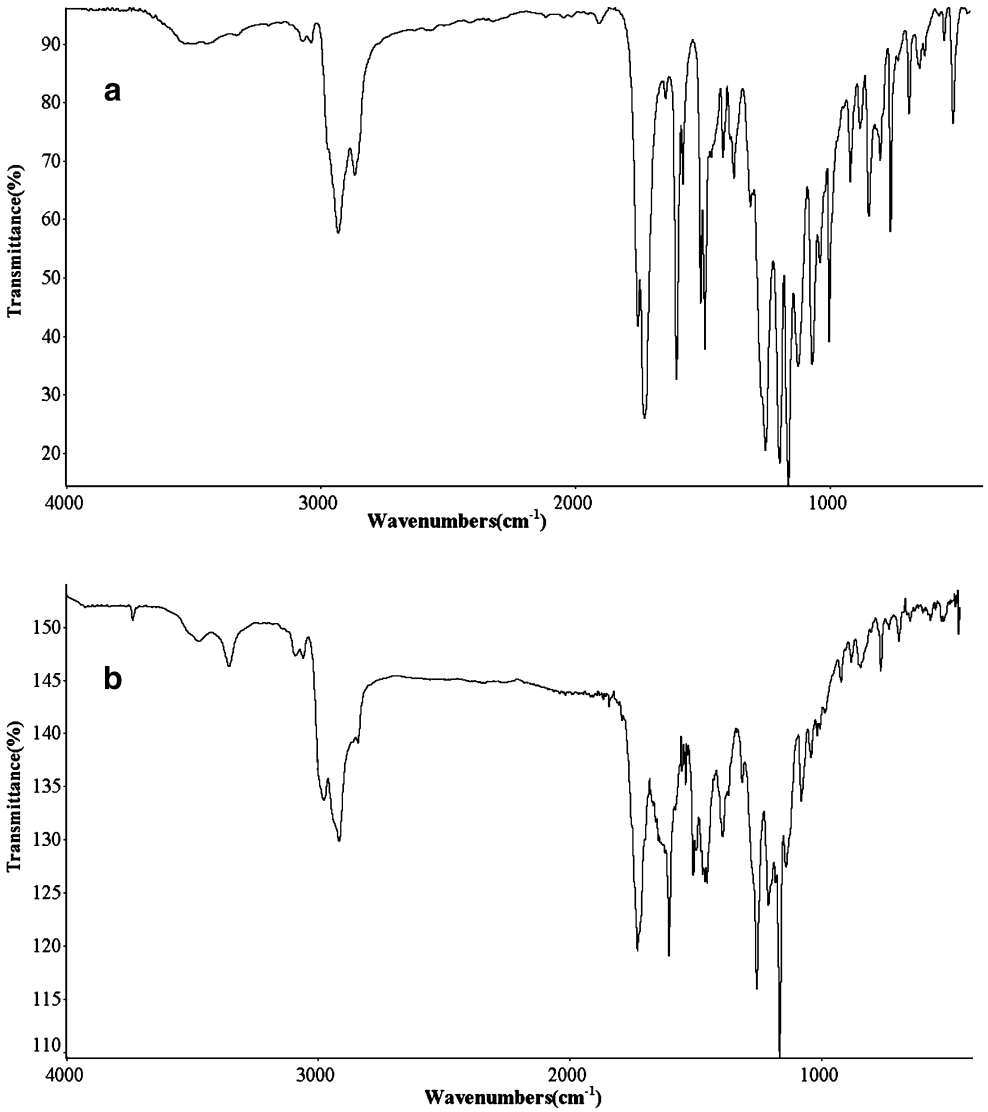

Fig. 1 FTIR spectrums of *M*-4 and *P*-4. (**a**) *M*-4; (**b**) *P*-4

16H, –Ar*H*–Ar*H*–), 1.55–2.35 (m, 16H, –OOC–(CH_2)$_4$–COO–), 0.95–4.05 (m, 37H, *H*–chenodiolyl), 11.73 (s, 1H, *H*O–chenodiolyl).

$4' - \text{hydroxybyphenyl} - 4 - \text{yl} - 4 - (\text{allyloxy})\text{benzoate}$ (5)

4-Allyloxybenzoic acid 4 and 4-allyloxybenzoyl chloride were prepared according to our previous paper [25]. The diphenol (36 g, 0.2 mol) was dissolved in THF (75 ml) and pyridine (15 ml), then 4-allyloxybenzoyl chloride (19.6 g, 0.1 mol) was slowly dropped into the above mixture at 0 °C. The mixture was stirred at room temperature for 4 h; thereafter it was refluxed for 22 h, and then it was poured into cool water. The precipitate was added to 5% NaOH aqueous solution (500 ml) to remove unreacted diphenol. The crude product was dried and recrystallized from mixed solvent of ethanol and acetone (mp: 192–194 °C, yield = 51%). IR (KBr, cm^{-1}): 3,447 (–OH); 3,078 (=C–H); 1,706 (–ArCOOAr–); 1,643 (C=C); 1,601; 1,491 (–Ar–); 1,262 (C–O–C). ^{1}H NMR ($CDCl_3$): 4.63 (d, 2H, J = 2.3Hz, –CH_2–CH=CH_2), 5.33 (d, 2H, J = 1.6Hz, –CH_2–CH=CH_2), 6.15 (m, 1H, –CH_2–C*H*=CH_2), 7.10 (d, 2H, J = 4.8Hz, –O–Ar*H*–COO–), 8.13 (d, 2H, J = 1.1Hz, –O–Ar*H*–COO–), 6.90–7.91 (m, 8H, –Ar*H*–Ar*H*–), 9.37 (s, 1H, Ar–O*H*).

$24 - [4' - \text{hydroxybiphenyl} - 4 - \text{yl} - 4 - (\text{allyloxy})\text{benzoyloxy}] - 3\alpha, 7\alpha - \text{di}$
$\{6 - [4' - (4 - \text{ethoxybenzoyloxy}) - \text{biphenyl} - 4 - \text{yloxy}] - 6 - \text{oxohexanoyloxy}\} - 5\beta - \text{cholane}(M - 4)$

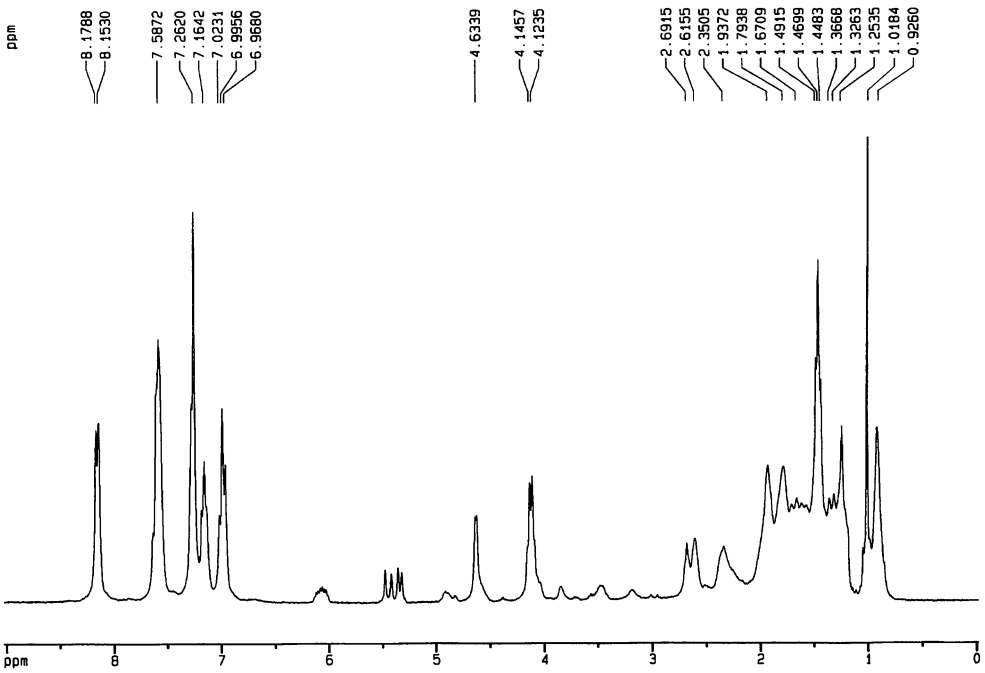

Fig. 2 ^{1}H NMR spectrum of M-4

The chenodeoxycholic acid derivative 5 (2.95 g, 2.3 mmol) was stirred in thionyl chloride (10 ml) and DMF (0.1 ml) as a catalyst was added. The solution was refluxed for 15 h whereby a clear solution was obtained. The excess of thionyl chloride was removed in vacuum for 4 h. For the esterification, the acid chloride was dissolved in dry chloroform (10 ml), and then dry pyridine (0.1 ml) and 4′-hydroxybiphenyl-4-yl-4-(allyloxy)benzoate (0.9 g, 2.4 mmol) was added. The reaction mixture was refluxed for 48 h in dry N_2 atmosphere. After cooling back to room temperature, the mixture was poured into cold water (150 ml) and acidified with hydrochloric acid. The precipitate was obtained by filtration and washed with distilled water. The pure product *M*-4 was obtained while hot to filter in acetone (mp: 207.5 °C, yield: 70%). IR (KBr, cm^{-1}): 2,933; 2,841 (–CH_2–); 1,741 (–RCOOAr–); 1,723 (–ArCOOAr–); 1,642 (C=C), 1602 (–Ar); 1,258 (C–O–C). ^{1}H NMR ($CDCl_3$): 1.33 (m, 6H, –CH_3), 4.12 (m, 4H, –OCH_2–), 7.16 (d, 4H, J = 5.0 Hz, –O–Ar*H*–COO–), 7.26 (d, 2H, J = 4.6 Hz, –O–Ar*H*–COO–), 8.15 (d, 2H, J = 1.1 Hz, –O–Ar*H*–COO–), 8.18 (d, 4H, J = 1.2 Hz, –O–Ar*H*–COO–), 7.16–7.59 (m, 24H, –Ar*H*–Ar*H*–), 1.67–2.35 (m, 16H, –OOC–(CH_2)$_4$–COO–), 0.93–4.01 (m, 37 H, *H*–chenodiolyl), 4.63 (d, 2H, J = 2.1 Hz, –CH_2–CH=CH_2), 5.31 (d, 2H, J = 1.5 Hz, –CH_2–CH=CH_2), 6.23 (m, 1H, –CH_2–C*H*=CH_2).

Polymers synthesis

The synthetic route of polymers is shown in Scheme 2. Because the synthesis procedure of polymers resembles that of the monomers, we choose polymer *P*–4 (n=4) to depict the synthesis procedure.

The compound *M*-4 (5.6 g, 3.5 mmol) was dissolved in dry toluene (30 ml). Azoisobutyronitrile (AIBN) (0.16 g, 1 mmol) as radical initiator was added to the stirred solution, and the mixture was heated to 60 °C under dry nitrogen atmosphere for 48 h. The polymer was obtained by precipitation in methanol, and then dried under vacuum. IR (KBr, cm^{-1}): 2,985; 2,844 (–CH_2–); 1,733 (–RCOOAr–); 1,719 (–ArCOOAr–); 1,607 (–Ar); 1,249 (C–O–C).

Results and discussion

Synthesis

Monomer *M*-4 and polymer *P*-4 are discussed here in detail to present the whole series due to their structure similarity;

Table 1 Phase transition temperatures of the *M*-*n* series

Monomer	Transition temperature/°C (corresponding enthalpy changes/J g^{-1}) heating/cooling	ΔT^a	ΔT^b	ΔT^c
M-0	$\frac{\text{K222.9(44.2)N305.1(0.8)I}}{\text{I298.3(−0.26)N200.1(−19.5)K}}$	82.2	98.2	317.0
M-4	$\frac{\text{K207.5(53.5)N304.2(0.1)I}}{\text{I298.6(−0.21)N180.5(−34.1)K}}$	96.7	118.1	310.0
M-8	$\frac{\text{K199.3(32.1)N300.4(0.6)I}}{\text{I292.2(−0.14)N170.1(−13.9)K}}$	101.1	122.1	315.0

K solid, *N* nematic, *I* isotropic

[a] Mesophase temperature ranges on first heating cycle

[b] Mesophase temperature ranges on first cooling cycle

[c] Temperature at which 5% weight loss occurred

Table 2 Thermal properties and specific rotation of the *P-n* series

Polymer	T_g(°C)	T_i(°C)	T^a(°C)	ΔT(°C)	$[n]^b$	$[a]_{589}^{20}$ (c 0.34, in $CHCl_3$)
P-0	108.3	199.1	255.0	90.8	0.15	−11.3
P-4	100.4	179.8	249.0	79.4	0.18	−25.9
P-8	75.1	162.7	247.0	87.6	0.19	−30.6

$\Delta T=(T_i-T_g)$
$[a]_{589}^{20}$: Specific rotation
[a] Temperature at which 5% weight loss occurred
[b] Intrinsic viscosity

the FTIR spectrums of *M*-4 and *P*-4 are shown in Fig. 1, and the ^{1}H NMR spectrum of *M*-4 is shown in Fig. 2. The FTIR spectrum of *M*-4 showed characteristic bands at 1,741–1,723 cm^{-1} originating from ester (C=O) stretching; 1,642 cm^{-1} was attributed to the presence of olefinic C=C stretching, 1,602 cm^{-1} was due to aromatic C=C stretching. The ^{1}H NMR spectrum of *M*-4 showed a series of multiple peaks at 7.16–8.18, 4.63–6.23, 1.33, 1.67–2.35, 4.12, and 0.93–4.01 ppm corresponding to aromatic, vinyl, methyl, methylene, methyleneoxy, and chenodeoxycholic acid protons. The new series of polymers were prepared by a one-step radical polymerization reaction between olefinic C=C of the monomer, using AIBN as radical initiator at 60 °C. The obtained polymers were insoluble in toluene, DMF, chloroform, etc., but swell in these solvents. The FTIR spectrum of *P*-4 showed the complete disappearance of C=C stretching band at 1,642 cm^{-1}. Characteristic absorption bands appeared at 1,719 and 1,607 cm^{-1} corresponding to the stretching of ester (C=O) and aromatic C=C, respectively.

Thermal properties

It is necessary to measure the phase transitions of monomer and polymer for many research works. The DSC measurement is a proper choice. The chain segment movement temperature of polymer from calm to moving is usually taken by the glass transition temperature (T_g), and the LC phase temperature from emerging to disappearing is taken by the isotropic transition temperature (T_i); T_g and T_i are important parameters for characterization and application.

The corresponding phase-transition temperatures of monomers are summarized in Table 1. According to the data, monomer *M-n* series show enantiotropic liquid crystalline behavior. The melting temperature (T_m) of monomer decreases from 222.9, 207.5, to 199.3 °C as the side-chain flexible space group extends (*n* increased from 0 to 8), and the mesophase temperature range of monomer increases as the flexible space group extends. This indicates the change of melting temperature and mesophase temperature range are in relation to length of flexible space group.

The corresponding phase-transitions temperatures of polymer *P-n* series are summarized in Table 2. These data are obtained during the second heating scan of the DSC, and the thermograms are shown in Fig. 3. It is evident that the T_i of *P-n* series decreases from 199.1 to 162.7 °C as the length of the side-chain flexible space group increases. The T_i is dependent on the length of the side-chain flexible space group significantly. Further, the T_g of *P-n* series also

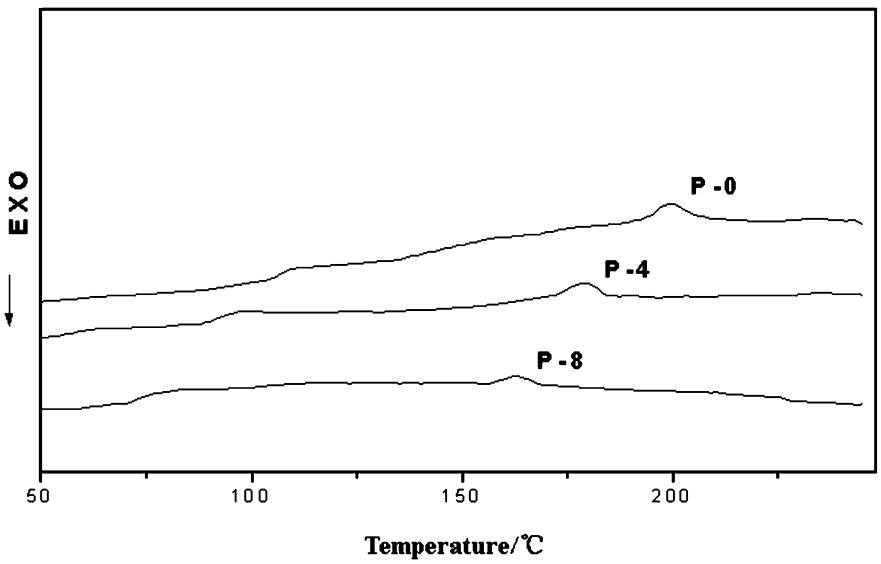

Fig. 3 DSC thermograms of the polymers

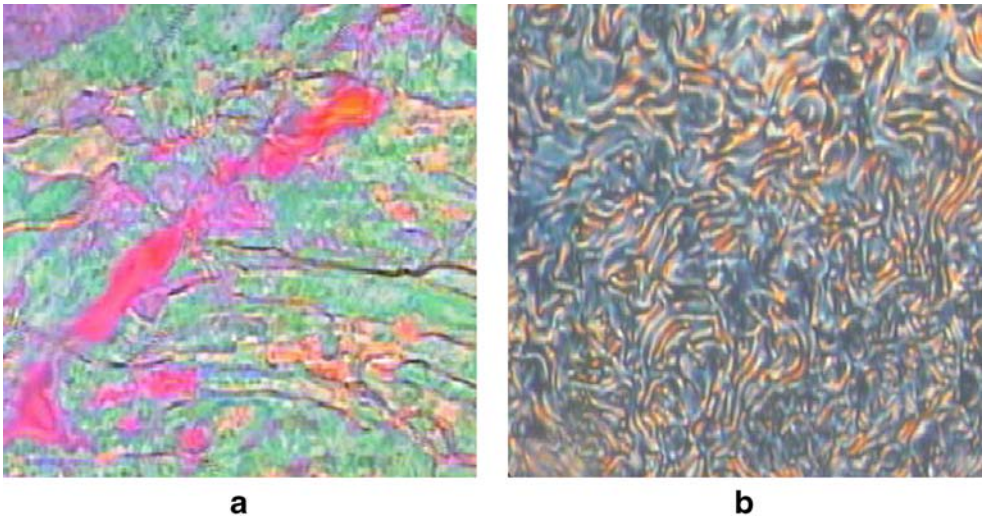

Fig. 4 Optical texture of *M*-4 and *P*-4 (200×). (**a**) Threadlike texture of *M*-4 in cooling to 262 °C; (**b**) threadlike texture of *P*-4 in heating to 148 °C

decreases from 108.3 to 75.1 °C as the number of methylene units in the side chain increases. However, the mesophase temperature range of *P-n* series does not extend as the flexible space group increases. All these observations of the thermal properties of *P-n* series indicate that the flexible space group in the side chain serves as diluent, the constraint on the motion of chain segments decreases and flexibility increases as flexible space group extends. Therefore, the phase-transition temperatures (T_g and T_i) decrease as the length of side-chain flexible space group extends.

The thermal stability of the obtained polymers has been evaluated by TGA in the N_2 atmosphere at a heating rate of 10 °C/min. It can show clearly the point and the degree of the polymer decomposition, and the results are shown in Table 2. The TGA results show that the temperatures at which 5% weight loss occurred (T^a) are higher than 245 °C for polymer *P-n* series. This indicates the synthesized polymers have relative high thermal stability. The relative high thermal stability is maybe caused by the bulky chenodiol group existing in the structure of polymers.

Texture analysis

The optical textures of monomer and polymer were studied by hot-stage POM. The POM observations showed that monomer and polymer all exhibited nematic threadlike texture during the heating and cooling cycles [26], and the phase-transition temperatures determined by DSC were consistent with POM observation results. The typical optical textures of *M*-4 and *P*-4 are shown in Fig. 4. When *P-n* series were heated to the glass transition temperature, the sample flowed quickly, the obvious threadlike texture appeared, and the texture did not change until the isotropic transition temperature. When the isotropic state was cooled from the isotropic phase, a droplet texture was observed at first, and then turned into a threadlike texture, which remained until the glass transition temperature. From the POM observations of the monomer and polymer we find that the expected cholesteric phase does not appear, indicating that the chenodeoxycholic acid units of *P-n* series cannot lead to formation of the cholesteric phase, although the cholesterol and chenodeoxycholic acid belong to the family of steroid compounds. This may be attributed to the lack of double bond (present in cholesterol) in the chenodeoxycholic acid units.

Although the change of space group length does not affect mesogenic type and texture of *P-n* series, the remarkable increase of SROT ($[a]_{589}^{20}$, temperature 20 °C, wavelength 589 nm) of *P-n* series is observed and summarized in Table 2. The SROT increases from $[a]_{589}^{20}$ −11.3 (*c* 0.34, in $CHCl_3$) to $[a]_{589}^{20}$ −30.6 (*c* 0.34, in $CHCl_3$) as the side-chain flexible space group extends; the reason is that the longer the linker between biphenyl unit and chenodiolyl, the more

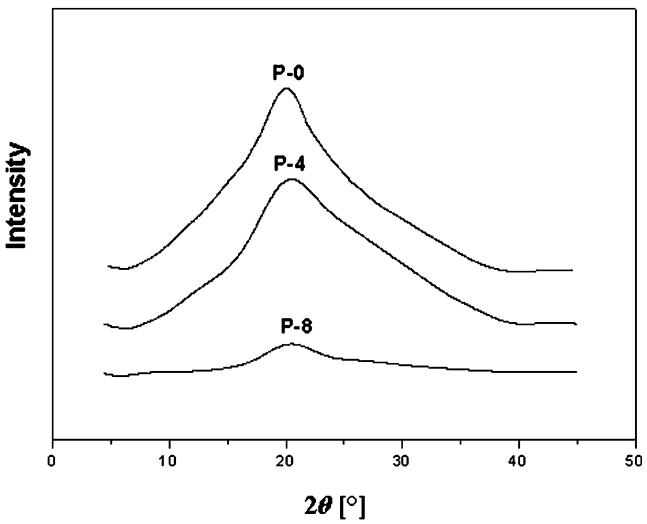

Fig. 5 X-ray diffraction patterns of quenched *P-n* series

freedom the chain has, the less compact the molecular packing.

X-ray diffraction

X-ray diffraction (XRD) studies were carried out to obtain more detailed information on structure parameter. In general, for smectic liquid crystalline phase, a sharp and strong peak at a low angle ($1°<2\theta<4°$) in small-angle X-ray scattering curve and a broad peak associated with lateral packing at $2\theta\approx20°$ can be observed in wide-angle X-ray diffraction curve. Whereas for nematic phase structure, no peak appears at a small angle, and a broad peak at $2\theta\approx20°$ can also be observed. For cholesteric phase structure, no peak appears at a small angle, and a broad peak occurs only at $2\theta\approx17.5°$ [25]. The XRD patterns of quenched polymers are shown in Fig. 5. All of the prepared polymers show amorphous diffuse peaks at about $2\theta\approx20°$, which can be attributed to the lateral spacing between the liquid crystalline molecules. No sharp peak in the lower Bragg angle region is observed. Combining POM with XRD measurement may reveal that the *P-n* series are nematic phase structure.

According to Fig. 5, the amorphous diffuse peaks of *P-n* series indicate an almost amorphous nature of the polymers. Further, the intensity of diffuse peak decreases with the flexible space group increases. This may be attributed to the longer side-chain degrading the arrangement of mesomorphic unit and short-range order parameter decreases.

Conclusions

A series of liquid crystalline monomers (*M-n* series) containing chenodiol units were prepared, these monomers were translated into side-chain liquid crystalline polymers (*P-n* series) by radical polymerization. These polymers showed good liquid crystalline behavior, and they enrich the theoretical research on side-chain liquid crystalline polymers. The *P-n* series demonstrated wide mesogenic region and high thermal stability, which offered the possibility of farther application in material field. The length of side-chain flexible space group played an important role in phase-transition temperatures of polymers: the glass transition temperature and isotropic transition temperature decreased as the side-chain flexible space group extended. The SROT of *P-n* series increased as the side-chain flexible space group extended. However, the length of flexible space group did not affect mesogenic type and texture of polymers. The typical nematic textures of monomer and polymer were observed, and nematic phase structure of *P-n* series was confirmed by POM and XRD.

Acknowledgment The authors are grateful to National Natural Science Fundamental Committee of China and HI-Tech Research and Development Program (863) of China for financial support of this work.

References

1. Mishra G, Srivastava AK (2007) Polym Bull 58:351
2. Kaneko K, Nakamura N (2007) Liq Cryst 34:229
3. Verploegen E, McAfee LC, Tian L, Verploegen D, Hammond PT (2007) Macromolecules 40:777
4. Singh R, Verploegen E, Hammond PT, Schrock RR (2006) Macromolecules 39:8241
5. Zhu ZG, Zhi JG, Liu AH, Cui JX, Tang H, Qiao WQ, Wan XH, Zhou QF (2007) J Polym Sci A Polym Chem 45:830
6. Millaruelo M, Chinelatto LS, Oriol L, Piñol M, Serrano JL, Tejedor RM (2006) Macromol Chem Phys 207:2112
7. Mishra G, Srivastava AK (2006) J Appl Polym Sci 102:4595
8. Ivanova R, Staneva R, Geppert S, Heck B, Walter B, Gronski W, Stühn B (2004) Colloid Polym Sci 282:810
9. Barmatov EB, Obrascov AA, Pebalk DA, Barmatova MV (2004) Colloid Polym Sci 282:530
10. Scheerder J, Marcelis ATM, Achten R, Sudhölter EJR (2000) Macromol Chem Phys 201:1303
11. Shibaev V, Bobrovsky A, Boiko N (2003) Prog Polym Sci 28:729
12. Zhao Y, Bai SY, Asatryan K, Galstian T (2003) Adv Funct Mater 13:781
13. Kago K, Seki T, Schücke RR, Mouri E, Matsuoka H, Yamaoka H (2002) Langmuir 18:3875
14. Park KH, Twieg RJ, Ravikiran R, Rhodes LF, Shick RA, Yankelevich D, Knoesen A (2004) Macromolecules 37:5163
15. Sainova D, Zen A, Nothofer HG, Asawapirom U, Scherf U, Hagen R, Bieringer T, Kostromine S, Neher D (2002) Adv Funct Mater 12:49
16. van Delden RA, Mecca T, Rosini C, Feringa BL (2004) Chem Eur 10:61
17. Zhang BY, Meng FB, Tian M, Xiao WQ (2006) React Funct Polym 66:551
18. Zhang JH, Bazuin CG, Freiberg S, Brisse F, Zhu XX (2005) Polymer 46:7266
19. Jia YG, Zhang BY, Sun QJ, Chang HX (2004) Colloid Polym Sci 282:1077
20. Ganicz T, Pakula T, Fortuniak W, Bialecka-Florjanczyk E (2005) Polymer 46:11380
21. Hu JS, Zhang BY, Tian M, Ren SC, Guo DY (2005) Colloid Polym Sci 283:1349
22. Hattori H, Uryu T (2000) J Polym Sci A Polym Chem 38:887
23. Pellicciari R, Costantino G, Camaioni E, Sadeghpour BM, Entrena A, Willson TM, Fiorucci S, Clerici C, Gioiello A (2004) J Med Chem 47:4559
24. Oishi T, Tsuchikawa H, Murata M, Yoshida M, Morisawa M (2004) Tetrahedron 60:6971
25. Zhang BY, Jia YG, Yao DS, Dong XW (2004) Liq Cryst 31:1
26. Dierking I (2003) Textures of liquid crystals, 1st edn. Wiley, New York